Two-dimensional discrete breathers: Construction, stability, and bifurcations

P. G. Kevrekidis,[1,2] K. Ø. Rasmussen,[1] and A. R. Bishop[1]
[1]*Theoretical Division and Center for Nonlinear Studies, Los Alamos National Laboratory, Los Alamos, New Mexico 87545*
[2]*Department of Physics and Astronomy, Rutgers University, 136 Frelinghuysen Road, Piscataway, New Jersey 08854-8019*
(Received 1 September 1999)

We develop a methodology for the construction of two-dimensional discrete breather excitations. Application to the discrete nonlinear Schrödinger equation on a square lattice reveals three different types of breathers. Considering an elementary plaquette, the most unstable mode is centered on the plaquette, the most stable mode is centered on its vertices, while the intermediate (but also unstable) mode is centered at the middle of one of the edges. Below the turning points of each branch in a frequency-power phase diagram, the construction methodology fails and a continuation method is used to obtain the unstable branches of the solutions until a triple point is reached. At this triple point, the branches meet and subsequently bifurcate into the final state of an extended phonon mode.

PACS number(s): 41.20.Jb, 63.20.Pw

In the past few years, the study of *intrinsic localized modes*, often referred to as *breathers*, has attracted considerable attention [1]. The existence of these modes has been proven rigorously for simple benchmark nonlinear systems such as diffusively coupled systems of pendula [2], while at the same time, they provide a natural channel for energy localization of interest to many branches of physics, as well as biology [3]. This appealing idea has guided much of the theoretical work towards testing such hypotheses in a number of systems of physical interest as the DNA double strand [4] or materials in the glassy state [5]. In fact recent experimental work [6] in these fields as well as in material science [7] seems to support this framework for energy trapping.

Although most of this methodology and associated theoretical techniques have been developed for the case of one spatial dimension, there have been some studies of higher-dimensional systems. Most importantly a rigorous proof of the existence of breathers in higher-dimensional nonlinear lattices was given in Ref. [2]. Also, the results of numerical studies have been published for several simple nonlinear lattices as for example two-dimensional Fermi-Pasta-Ulam chains [8,9], Klein-Gordon chains [10] and also for DNLS systems [11,12]. Systems of higher dimensionality have also been investigated [13].

Most experimental systems of interest are not one-dimensional, necessitating generalizations to higher spatial dimensions, such as the ones mentioned above. In the perspective of the need to identify the similarities as well as differences between one and higher spatial dimensions, we give here a synopsis of our results on the construction, behavior and stability of breathers in two dimensions.

The system we study is the discrete nonlinear Schrödinger (DNLS) equation

$$i\dot{u}_{i,j} = -k\Delta_2 u_{i,j} - |u_{i,j}|^2 u_{i,j}, \tag{1}$$

where $\Delta_2 u_{i,j} = u_{i+1,j} + u_{i-1,j} + u_{i,j+1} + u_{i,j-1} - 4u_{i,j}$ is the second order difference operator in two spatial dimensions and the overdot denotes partial differentiation with respect to time. The motivation for studying this model is twofold. First, the DNLS finds applications in almost all of the above mentioned physical settings. Secondly, the DNLS is a generic envelope equation describing to leading order the behavior of solitons in, for example, Klein-Gordon lattices.

The breather construction technique we employ has been described previously [14] and we will only briefly review it here. We use an ansatz $u_{i,j} = \exp(-i\Lambda t)\psi_{i,j}$ for the solution of Eq. (1) and obtain the two-dimensional steady state equation

$$\Lambda \psi_{i,j} = -k\Delta_2 \psi_{i,j} - |\psi_{i,j}|^2 \psi_{i,j}. \tag{2}$$

This equation (see also Ref. [15]) is, in essence, a nonlinear eigenvalue problem. Hence, taking advantage of a Rayleigh-Ritz variational principle type formalism we can construct the ground state solution iteratively. Given an initial condition, the matrix $[H]$ is constructed as

$$[H]_{m,m} = 4k - |\psi_{i,j}|^2, \tag{3}$$

$$[H]_{m,m+1} = [H]_{m,m-1} = [H]_{m,m+N} = [H]_{m,m-N} = -k, \tag{4}$$

where $m = i + (l-1)j$, $l = 1,2,\ldots,N$ for lattices of size $N \times N$. Equation (4) is given with the understanding that for $i = 1$ and N the chosen boundary conditions have to be implemented. Solving the remaining linear eigenvalue problem refines the prediction of $\psi_{i,j}$ (as the eigenfunction corresponding to the most negative eigenvalue). This procedure is repeated until the desired precision is reached. The advantage of this method is that it is faster and easier to implement than full limit-cycle integration [16], used in conjunction with Newton-Raphson iterative refinement of the solutions obtained at the cross section of the Poincare map.

In this fashion, the three branches, shown in Fig. 1, with symbols (triangles, stars, circles) have been constructed. We will refer to these branches as *primary* because the modes residing on them can be tracked by our technique. Each branch corresponds to a family of breathers having identical symmetry properties. In Fig. 1 each family is characterized by the relation between the frequency Λ and the *power*

$$P = \sum_{i,j} |\psi_{i,j}|^2. \tag{5}$$

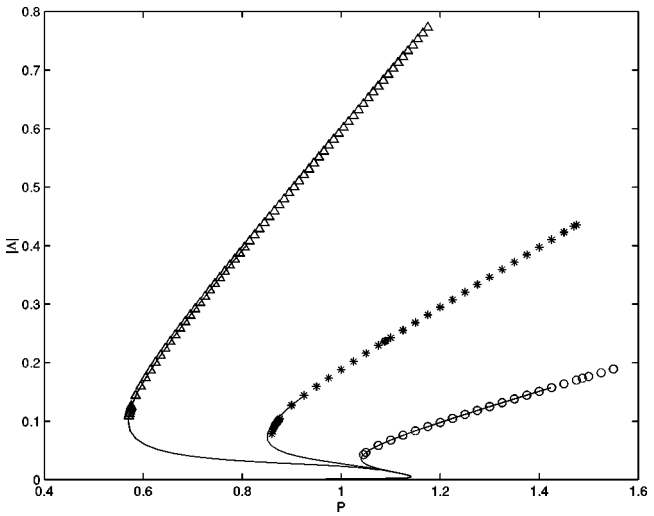

FIG. 1. Bifurcation diagram of frequency vs power. Solid lines calculated via continuation, symbol lines via our technique. See text for detailed explanation.

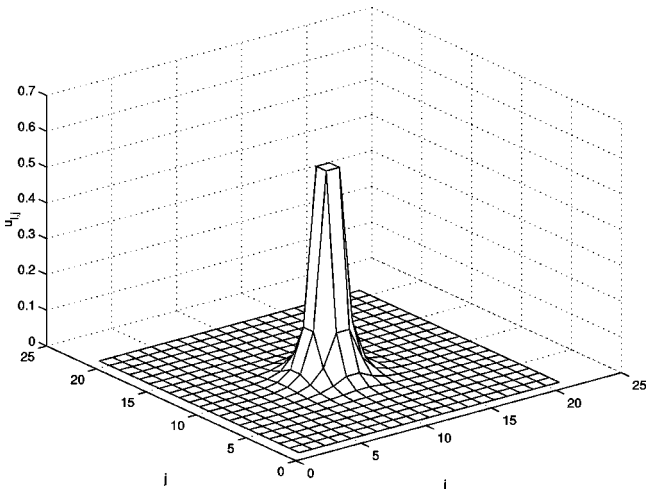

FIG. 3. Spatial profile of a Page-like mode.

It is known that there are many [8] breather configurations (in fact infinitely many if one invokes the ''multibreather'' concept [17]). We will however focus our attention on the three most simple configurations shown in Fig. 1.

(1) A mode centered on a vertex of a plaquette (i.e., a lattice site). This mode corresponds to the Sievers-Takeno (ST) mode [18] in one dimension (1D). An example of such a mode is given in Fig. 2.

(2) A mode centered on the center of the plaquette corresponding to the Page mode in 1D [19], as shown in Fig. 3.

(3) Finally, Fig. 4 depicts a hybrid mode with no 1D equivalence. Along one direction this mode is centered on a site, while along the other direction it is centered between sites. This hybrid mode is thus centered at the middle of any one of the edges of the plaquette.

Clearly, there is one Page-like mode per plaquette, and also four ST-like modes in each plaquette, but each belongs to four plaquettes, such that their multiplicity is also unity. However, the multiplicity of the four hybrid modes is two, since there is the possibility of one in each direction (alternatively each of the four belongs to two squares). Viewing these branches in the perspective of a bifurcation diagram, allows two possible descriptions. First, placing a horizontal cut along the $(|\Lambda|,P)$ diagram, shows that to each value of the frequency Λ corresponds three modes with different powers, P. The values of P for the three modes range from one where the power is practically stored on a single site (low power, ST-like mode), via an intermediate mode (power stored in two sites, hybrid mode), to a high power mode where the power is stored on four sites (Page-like mode).

Second, noticing that the frequency $|\Lambda|$ is related to the energy through the equation $E=P\Lambda+\frac{1}{2}\Sigma|\psi_{i,j}|^4$, allows a second interpretation. Namely, considering the primary branches, three possibilities for each value of the power (i.e.. for a vertical cut in the phase plane) appear. (1) The lowest energy mode corresponds to the ground state of the system and is the ST-like mode. (2) The first excited state corresponds to the hybrid mode. (3) The second excited and most unstable state corresponds to the Page-like mode.

This second description is more common in the 1D problem, in the sense that the difference in energy between these modes relates to a Peierls-Nabarro (PN) barrier [20], which,

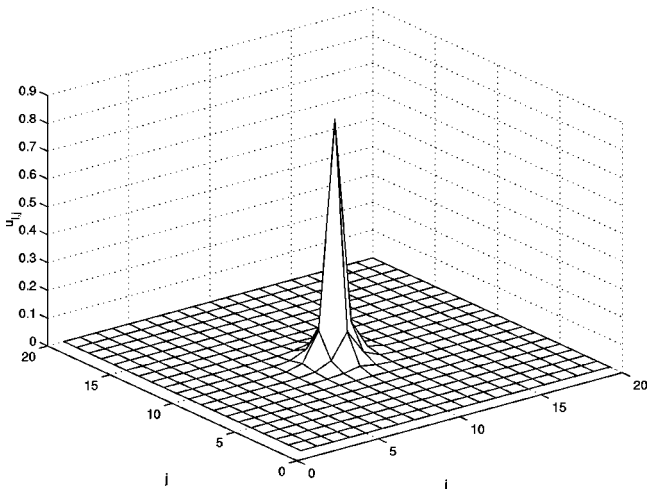

FIG. 2. Spatial profile of a Sievers-Takeno-like mode.

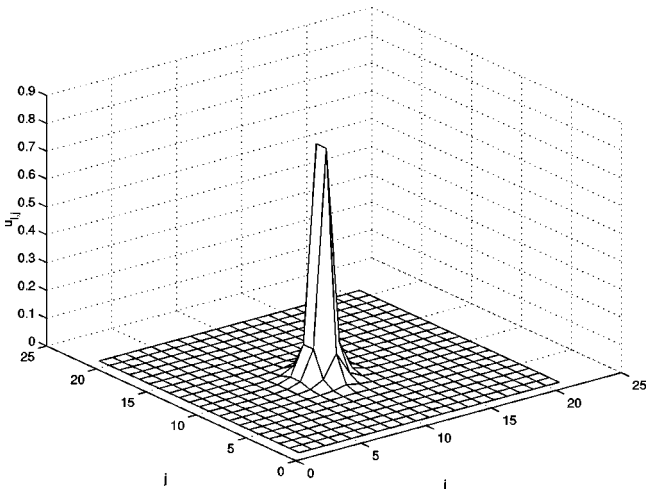

FIG. 4. Spatial profile of a hybrid mode.

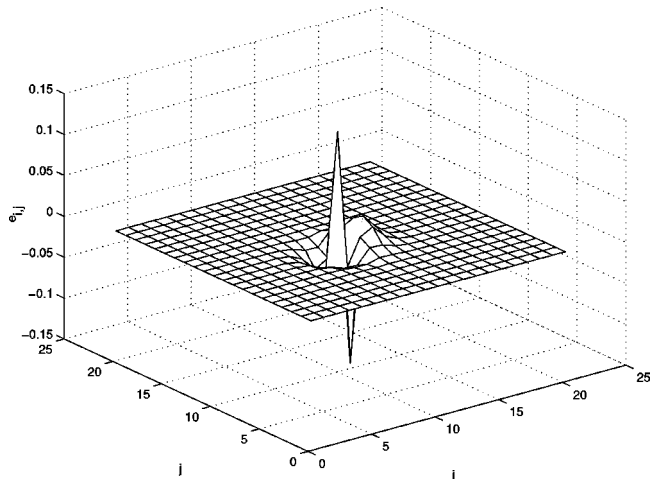

FIG. 5. Antisymmetric unstable eigenmode spatial profile in the hybrid case.

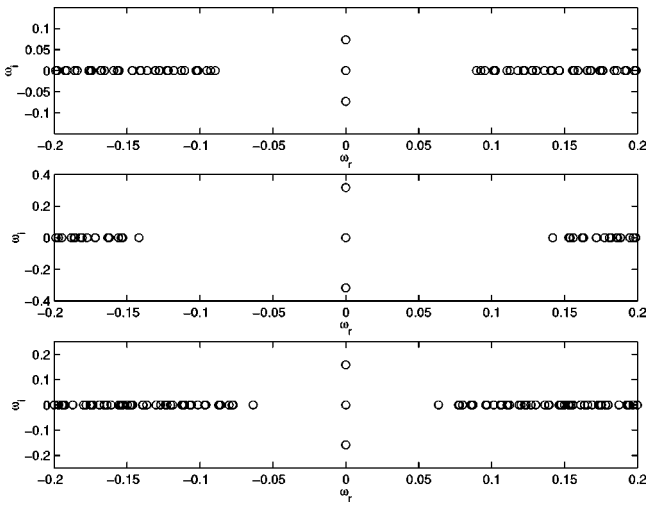

FIG. 6. Sample calculations of eigenvalue spectra. The spectral plane is shown for the three cases identified in the text.

roughly, corresponds to the energy an unstable mode should release in order to gain stability. The stability of these modes has been extensively studied within the framework of linear stability analysis. Again, the main advantage, provided by the gauge symmetry of the DNLS, is that linear stability can be studied within the rotating wave approximation (see, e.g., Ref. [21]). We substitute the ansatz $u_{i,j}=\exp(-i\Lambda t)(\psi_{i,j}+\epsilon v_{i,j})$ into Eq. (1) and using the fact that ψ is the solution of Eq. (2) we get that the perturbation $v_{i,j}$ satisfies (see, e.g., Ref. [22])

$$i\dot{v}_{i,j}+k\Delta_2 v_{i,j}+2|\psi_{i,j}|^2 v_{i,j}+\psi_{i,j}^2 v_{i,j}^{\star}+\Lambda v_{i,j}=0. \quad (6)$$

Further, the ansatz $v_{i,j}=a_{i,j}\exp(-i\omega t)+b_{i,j}\exp(i\omega t)$, leads to

$$\omega a_{i,j}=-k\Delta_2 a_{i,j}-2|\psi_{i,j}|^2 a_{i,j}-\Lambda a_{i,j}-\psi_{i,j}^2 b_{i,j}^{\star}, \quad (7)$$

$$-\omega b_{i,j}=-k\Delta_2 b_{i,j}-2|\psi_{i,j}|^2 b_{i,j}-\Lambda b_{i,j}-\psi_{i,j}^2 a_{i,j}^{\star}. \quad (8)$$

From Eqs. (7) and (8) it is found that the ST-like mode always is stable on the primary branch [e.g., all eigenvalues of Eqs. (7) and (8) are positive]. On the contrary, for the hybrid mode (on the primary branch) one eigenvalue exists on the imaginary axis and causes this mode to be unstable (an example of the spatial configuration of the eigenfunction corresponding to this eigenvalue is given in Fig. 5). Finally, the Page-like mode is much more unstable in the sense that it generically has three imaginary eigenvalues. Since the system possesses time reversal symmetry, the eigenvalues appearing on the positive branch of the axis always have time reversal symmetric partners on the negative branch. A pair among them has the same frequency (because of the fourfold rotational symmetry), while the eigenfunctions corresponding to these modes are spatially antisymmetric.

The termination of each of the primary branches comes about through a saddle-node bifurcation which is exactly the type of behavior we have found to be generic in 1D systems [23,24]. However, in our present 2D case the bifurcation structure is much richer. In particular, in the case of the ST-like mode around $P\approx 0.58$ a spatial mode with symmetry of the breather bifurcates from the edge of the phonon band and enters the origin of the spectral plane at $P\approx 0.57$, giving rise to the first turning point, thereafter existing along the pure imaginary axis [see, e.g, Fig. 6(a)]. A similar scenario (i.e., a mode with the spatial symmetry of the breather bifurcates from the band edge and enters the origin), appears in the case of the hybrid mode.

The bifurcation from the band edge occurs in this case at $P\approx 0.927$ [Fig. 6(b)] and the saddle-node occurs at $P\approx 0.851$. Finally, in the case of the Page-like mode, the single antisymmetric mode (out of the three that originally resided on the imaginary axis) bifurcates along the real line [Fig. 6(c)] at $P\approx 1.1385$ but through a new bifurcation returns to the imaginary axis, giving rise to the turning point at $P\approx 1.04$. This scenario (of different excitation power thresholds for the different modes), is consistent with the recent predictions of Refs. [15,12] for the existence of such thresholds, for lattices with dimensionality higher than 1. In fact, the theoretical expression for these thresholds that are given in Ref. [15] depends on the spatial profile of the mode, thus justifying our finding that the thresholds depends on the shape of the discrete modes. The very rich structure of the *secondary* branches (i.e., beyond the turning points) has been followed through continuation methods, as will be described in detail elsewhere. However, the final fate of the three modes can be seen in Fig. 1; they merge in what appears to be a triple point and finally bifurcate to an extended phonon mode $P\approx 1.142$, $|\Lambda|\approx 0.0051$ [26]. It is worth noticing that this value is in exact agreement with the continuum result for the localized ground state in 2D [25].

In summary we have presented detailed investigations of the structure and stability of two-dimensional breather modes on a square lattice in the framework of the discrete nonlinear Schrödinger equation. We have found interesting differences between two dimensions and some results found in the context of one spatial dimension. These differences arise through the existence of a hybrid mode, as well as from a much richer stability scenario. This picture has been characterized using bifurcation theory tools and continuation meth-

ods. We believe that the subtleties of discrete nonlinear lattice solutions, accessible through the methodologies presented here, will be of value for developing theoretical frameworks. They should also be of value to experimentalists, for quantitative guidance in a much wider range of 2D systems, to which energy localization may be relevant.

P.G.K. gratefully acknowledges the hospitality of the Theoretical Division and the Center for Nonlinear Studies at the Los Alamos National Laboratory, as well as support from the ''A.S. Onassis'' Public Benefit Foundation. Research at Los Alamos National Laboratory is performed under the auspices of the U.S. DOE.

[1] See, e.g., Physica D **119**, 1 (1998).
[2] R. S. MacKay and S. Aubry, Nonlinearity **7**, 1623 (1994).
[3] See, e.g., Physica D **68**, 1 (1993).
[4] M. Peyrard and A. R. Bishop, Phys. Rev. Lett. **62**, 2755 (1989).
[5] G. Kopidakis and S. Aubry, Physica D **130**, 155 (1999).
[6] A. Campa and A. Giasanti, http://xxx.lanl.gov/abs/physics/9802043.
[7] B. I. Swanson, J. A. Brozik, S. P. Love, G. F. Strouse, A. P. Shreve, A. R. Bishop, W. Z. Wang, and M. I. Salkola, Phys. Rev. Lett. **82**, 3288 (1999).
[8] F. Fisher, Ann. Phys. (Leipzig) **2**, 296 (1993).
[9] S. Takeno, J. Phys. Soc. Jpn. **61**, 2821 (1992); S. Flach, K. Kladko, and S. Takeno, Phys. Rev. Lett. **79**, 4838 (1997).
[10] V. M. Burlakov, S. A. Kiselev, and V. N. Pyrkov, Phys. Rev. B **42**, 4921 (1990); S. Flach, K. Kladko, and C. R. Willis, Phys. Rev. E **50**, 2293 (1994); J. M. Tamga, M. Renmoissenet, and J. Pouget, Phys. Rev. Lett. **75**, 357 (1995).
[11] J. Pouget, M. Remoissenet, and J. M. Tamga, Phys. Rev. B **47**, 14 866 (1993).
[12] S. Flach, K. Kladko, and R. S. MacKay, Phys. Rev. Lett. **78**, 1207 (1997).
[13] D. Bonart, A. P. Mayer, and U. Schröder, Phys. Rev. Lett. **75**, 870 (1995); S. A. Kiselev and A. J. Sievers, Phys. Rev. B **55**, 5755 (1997).
[14] P. G. Kevrekidis, K. Ø. Rasmussen, and A. R. Bishop, Phys. Rev. E (to be published).
[15] M. I. Weinstein, Nonlinearity **12**, 673 (1999).
[16] J. L. Marin and S. Aubry, Nonlinearity **9**, 1501 (1996).
[17] S. Aubry, Physica D **103**, 201 (1997); D. Chen, S. Aubry, and G. P. Tsironis, Phys. Rev. Lett. **77**, 4776 (1996).
[18] A. J. Sievers and S. Takeno, Phys. Rev. Lett. **61**, 970 (1988).
[19] J. B. Page, Phys. Rev. B **41**, 7835 (1990).
[20] Yu. S. Kivshar and D. K. Campbell, Phys. Rev. E **48**, 3077 (1993).
[21] K. W. Sandusky, J. B. Page, and K. E. Schmidt, Phys. Rev. B **46**, 6161 (1992).
[22] M. Johansson and S. Aubry (unpublished).
[23] D. Cai and P. G. Kevrekidis (unpublished).
[24] P. G. Kevrekidis, K. Ø. Rasmussen, and A. R. Bishop (unpublished).
[25] P. L. Christiansen, Yu. B. Gaididei, K. Ø. Rasmussen, V. K. Mezentsev, and J. Juul Rasmussen, Phys. Rev. B **54**, 900 (1996).
[26] For all calculations in this paper we have chosen $k=0.1$. Although the specific values at which the bifurcations occur depend on this parameter, the features will remain unchanged.